

FACTORS INFLUENCING RESPONSE TIME OF DEP MICROFLUIDIC ACTUATION

T. B. Jones¹, T. Ito², H. Yoo¹, and R. Ahmed¹

¹ University of Rochester, Rochester, NY (USA)

² Toba National College of Maritime Technology, Toba (Japan)

Abstract

Dielectrophoretic (DEP) microfluidic actuation features rapid on-chip manipulation, picoliter droplet dispensing, and mixing of aqueous liquids. In droplet dispensing applications, two critical time scales are identified: (i) the time required to fill the flow structure when voltage is applied and (ii) the time required for the capillary instability to form droplets after voltage is removed. For $\sim 10 \mu\text{m}$ flow structures, filling takes much longer than droplet formation.

Keywords: microfluidics, laboratory-on-a-chip, dielectrophoresis, electrowetting

1. Introduction

DEP microfluidic actuation utilizes dielectric-coated, coplanar electrodes excited by AC voltage to pattern non-uniform electric fields for liquid manipulation on open substrates. It exploits the attractive tendency of dielectric liquids toward regions of stronger electric field. Fig. 1 shows a typical flow structure in cross-section. DEP microactuation is related to electrowetting [1], differing primarily in that DEP uses AC voltage at sufficient frequency so that the electric field penetrates the liquid and controls its shape [2]. In contrast, electrowetting uses DC voltage (or low frequency AC), meaning that free electric charge builds up on the surface and alters the contact angle but not the liquid profile.

DEP is fast, an important attribute in certain μTAS applications; in some cases, the leading edge of a finger is observed to move at speeds of $\sim 50 \text{ cm/s}$. However, the transient fluid mechanics that control droplet dispensing are not well-understood, so we are using a high-speed video camera to record and study the behavior. Fig. 2 shows selected frames from a video of a liquid finger on a co-planar electrode structure like Fig. 1. The microscope is trained downward

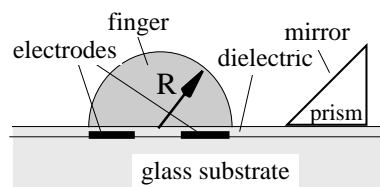


Fig. 1. Cross-sectional view of the coplanar electrodes, showing profile of liquid contained by DEP force. Liquid flows into or out of plane of paper. Mirror placed beside structure permits side view of moving finger.

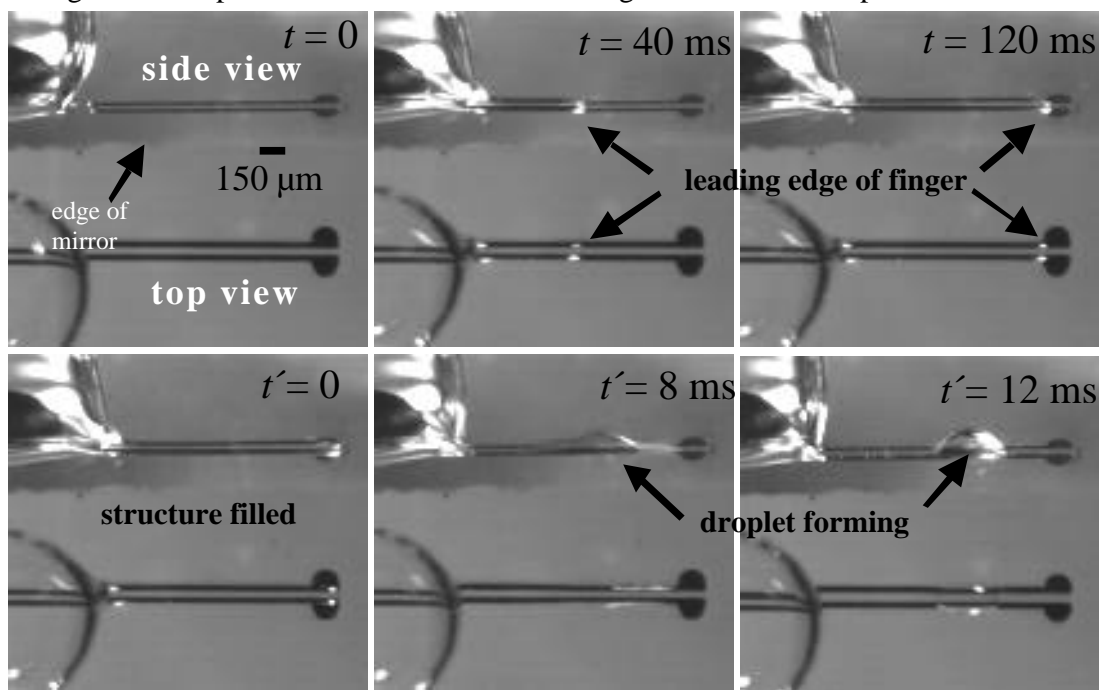


Fig. 2. Selected frames from video sequence (250 fps) showing (i) movement of finger in oil bath when voltage is applied at $t = 0$ and (ii) formation of a droplet when voltage is removed shortly after $t' = 0$.

on the horizontally oriented substrate. A mirror positioned at a 45° angle on the substrate alongside the electrodes allows simultaneous viewing from the side. When AC voltage is applied at $t = 0$ s, the finger emerges from the microliter-sized reservoir droplet of de-ionized water at the left, moves rapidly to the right, and stops at the end of the electrodes. When voltage is removed, two things happen: (i) the capillary force starts to draw the finger back into the large droplet and (ii) the capillary jet instability deforms the surface and pinches off a droplet. For the structure in Fig. 2, which has electrodes of width $50 \mu\text{m}$, spacing $50 \mu\text{m}$, and length 3 mm , typically only one or two droplets form. On the other hand, for structures with feature size down to $\sim 10 \mu\text{m}$, the capillary instability overwhelms capillary-driven finger retraction, making it possible to dispense multiple droplets in the ~ 50 picoliter volume range.

2. Dynamics of finger motion

Reviewed here is a simple model for the transient dynamics, wherein we assume that the cross-sectional profile of the advancing finger is semicircular (radius R), and constant along its length. Momentum may be ignored and so the force balance on a control volume containing the finger yields

$$f^e + f + f_\mu = 0 \quad (1)$$

The DEP and surface tension forces, $f^e = V^2 dC/dZ$ and $f = -R$, respectively, are constant, and the drag force, $f_\mu = -2RZ\mu$, is area-dependent. $C(Z)$ is the system capacitance, V is rms-applied voltage, and μ is the surface tension. Assume viscous shear is proportional to finger velocity, i.e., $\mu = KdZ/dt$, where K is a proportionality factor dependent on radius R and liquid viscosity μ . The solution to Eq. (1) takes the form: $Z(t) \propto \sqrt{t}$.

Representative experimental data for a water finger in air, along with a fitted square-root law curve, are plotted in Fig. 3. For the curve, the so-called dielectric thickness d/d_0 (where d is the thickness of the dielectric coating and d_0 is the dielectric constant) was used as an adjustable parameter. A best fit is achieved for $d/d_0 = 2.17$, whereas, if we use $d = 10 \mu\text{m}$ and $d_0 = 3$ (for polyimide), the correct value should be 3.33 . Factors contributing to this discrepancy include electrical breakdown in the dielectric and uncertainties about the experimental parameters.

For experiments performed in oil, the transient motion of a water finger is smoother and good actuation is achievable at lower frequencies. This performance enhancement may result from the oil film that lubricates the finger. Heating effects are diminished because of heat transfer to the oil. It should be noted, however, that the cross-section of the moving finger is no longer uniform along its length, making application of the above model invalid for this case.

3. Droplet formation dynamics

Droplets form when the voltage is removed because, without the non-uniform AC electric field to stabilize the hydrostatic equilibrium, the capillary instability takes over. For structures with $>50 \mu\text{m}$ cross-sections immersed in oil (cf., Fig. 2), this instability, which breaks up the finger into droplets, and surface tension, which tries to retract the liquid finger, compete after voltage removal. We estimate that, for larger structures, 50% or more of the liquid is returned to the reservoir droplet. By contrast, we believe thinner structures retain most of the liquid after voltage is removed, but because the finger is slower to fill, there is typically much less liquid distributed along the structure when the voltage is removed. This leads to formation of large numbers of small droplets. Fig. 4 shows 26 droplets, ranging in volume from ~ 20 to ~ 70 picoliters, distributed along a ~ 35 micron wide, $\sim 6 \text{ mm}$ long structure. In this experiment, the droplets formed in $\sim 2 \text{ ms}$, while it took $\sim 300 \text{ ms}$ for the finger to reach the end of the structure.

One may test the correspondence of droplet spacing to the fastest growing wavelength as predicted by hydrodynamic theory. The mean spacing for the droplets in Fig. 4 is $200 \mu\text{m}$ ($\pm 58 \mu\text{m}$), while the theory of rivulets predicts $143 \mu\text{m}$ [3]. This probably stems from the questionable assumption that the finger profile is semicircular, though the influence of oil viscosity may also be substantial. The speed and physical dimensions involved make determination of the time-dependent profile of the finger very difficult.

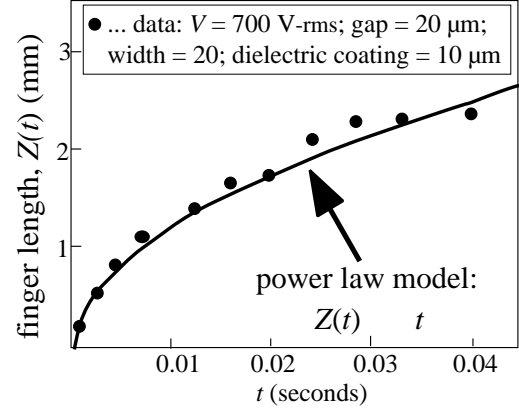


Fig. 3. Finger length Z versus time t for a de-ionized water finger in air. Plotted curve is the best-fit curve for $Z(t) \propto \sqrt{t}$.

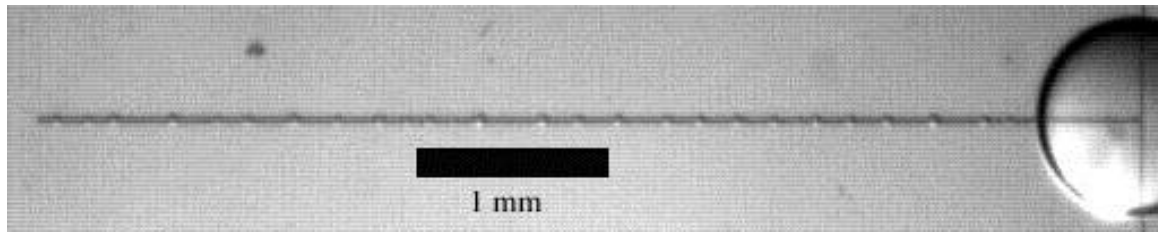


Fig. 4. Dispensing of 26 droplets with volume ranging from ~20 to ~70 picoliters (average ~ 37 picoliters) on co-planar strip electrodes (evaporated Al on glass): width $w = 10 \mu\text{m}$, spacing $g = 16 \mu\text{m}$. Experimental liquid: DI water in an oil bath. Dielectric coating: ~1.5 μm of spin-coated photoresist (Shipley #1805) applied in two layers with very thin, intervening layer of Teflon AFTM. Volume of reservoir droplet at right is ~1 microliter.

4. Discussion

Substituting ethylene glycol for water in the oil bath experiment provides an instructive example of the interplay of the two time scales. In this case, the finger does not break up into droplets when the voltage is turned off, but instead remains intact and withdraws smoothly back into the reservoir droplet. Instability is almost entirely suppressed, presumably because the interfacial tension of ethylene glycol against oil (~0.02 Nt/m) is about one-fourth the water/oil value. Reduced interfacial tension increases the minimum unstable wavelength and decreases the unstable growth rate. The increased viscous drag due to the oil also inhibits the instability.

5. Conclusion

On-chip, DEP droplet dispensing speed is controlled by the time required to fill the electrode structure rather than by the hydrodynamic instability that actually forms the droplets. Thus, making DEP droplet dispensing accurate and reliable requires better knowledge of the dynamics of the finger. It is clear that many factors influence these dynamics, including the dielectric constant and thickness of the insulating coating, the interfacial tension and viscosity of the liquid, the wetting properties of the dielectric, and the structure dimensions. At least for actuation of water in air, the $Z(t) \propto \sqrt{t}$ law can be used to estimate scaling factors. For example, doubling the electrode length increased the filling time by a factor of four. Compared to most microfluidic schemes, DEP actuation is very fast; however, this scaling law imposes strict limits relating speed to the size of structures. In the case of DEP actuation in insulating oil, the fluid dynamics are far more complex. Numerical modeling will be required to establish the scaling law.

There are other important time scales that influence DEP actuation. For example, even DI water tends to heat up. We have seen instances where the leading edge of a finger starts to boil if it moves too slowly. The leading edge boils first because it is subjected to Joule heating for the longest time. Increasing the voltage to speed up the finger reduces exposure time of the water to the electric field and alleviates boiling. But increasing the voltage can lead to another problem: electrical breakdown. Practical μTAS applications of DEP involve optimization with respect to materials properties including dielectric constant, breakdown resistance, and wetting properties.

Acknowledgments

The National Science Foundation (USA), the National Institutes of Health (USA), and the Center for Future Health (University of Rochester) supported this work. T. Ito acknowledges a fellowship from the Ministry of Education, Culture, Sports, Science and Technology (Japan). M. Gunji, R. Mulgund, D. Hsu, and P. Osborne assisted with the experiments.

References

1. B. Berge, "Électrocapillarité et mouillage de films isolants par l'eau," *C. R. Acad. Sci. Paris, Série II*, 157-163 (1993); M. G. Pollack, R. B. Fair, A. D. Shenderov, "Electrowetting-based actuation of liquid droplets for microfluidic actuation," *Applied Physics. Lett.* **77**, 1725-1726 (2000); J. Lee, H. Moon, J. Fowler, T. Schoellhammer, and C-J. Kim, *Sensors and Actuators A* **95**, 259-268 (2002).
2. T. B. Jones, M. Gunji, M. Washizu, and M. J. Feldman, "Dielectrophoretic liquid actuation and nanodroplet formation," *J. Applied Physics* **89**, 1441-1448 (2001).
3. S. Schiaffino and A. A. Sonin, "Formation and stability of liquid and molten beads on a solid surface," *J. Fluid Mech.* **343**, 95-110 (1997).